

Symbolic Analysis Using Floating Pathological Elements

Hung-Yu Wang^{1,*}, Shung-Hyung Chang², Nan-Hui Chiang¹, and Quoc-Minh Nguyen¹

¹Department of Electronic Engineering, National Kaohsiung University of Applied Sciences, Kaohsiung, Taiwan, R.O.C.

²Department of Microelectronics Engineering, National Kaohsiung Marine University, Kaohsiung, Taiwan, R.O.C.
hywang@kuas.edu.tw

Abstract. The nullor-mirror pathological elements have been found useful in solving circuit analysis and design problems. They are further used to ideally represent various popular analog signal-processing properties that involve differential or multiple single-ended signals by utilizing the concept of floating mirror elements. For applying nodal analysis to the circuit containing such active devices with differential or multiple single-ended signals, we propose an efficient systematic analytical technique which directly performs symbolic analysis on the simpler RLC-nullor-floating mirror representations of circuits rather than their RLC-two-terminal pathological element-based counterparts. It releases the limitation of recently proposed symbolic analysis approaches and use simpler models which may be conducive to achieving high-performance symbolic nodal analysis. The feasibility and validity of the proposed method are demonstrated by practical circuit examples.

Keywords: Pathological element, RLC-nullor-floating mirror network, nodal analysis (NA), symbolic analysis.

1 Introduction

Tellegen first implicitly introduced a minimum-sized set of ideal elements in 1954 with which any linear and nonlinear driving-point impedance or transfer characteristic can be synthesized, and it is given the name of nullor by Carlin ten years later [1]-[2]. Since then, nullor has been accepted within the network theory community as a basic network element and it has been proven to be a very valuable network analysis, synthesis and design tool [3]-[5]. Recently, the mirror elements with grounded reference node have been extended to include the floating mirror elements [6]-[7]. With such extensions, a nullator and a norator can be represented in terms of a floating voltage mirror and a floating current mirror, respectively [8]. Moreover, the floating mirror elements are used to derive the pathological sections which ideally represent various popular analog signal-processing properties that involve differential

* Corresponding author.

or multiple single-ended signals; like conversion between differential and single-ended voltages, differential voltage conveying and current replication. In virtue of the combination of various pathological sections, they are used to model many popular active devices, such as the differential voltage current conveyor (DVCC), the fully differential second generation current conveyor (FDCCII) and two-output CCII and ICCII family [7]-[9]. Since the better flexibility and simpler configuration of modeling active devices using the combination of nullor mirror elements, the pathological representations of many active devices have been reported in the literature [10]-[11].

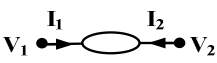

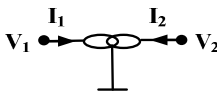
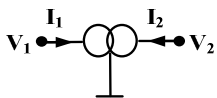
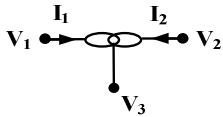
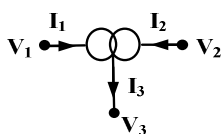
To make good use of the simpler RLC-pathological element-based networks, a systematic analytical technique which performs direct analysis for nullor-mirror equivalent networks has been reported, and its improvement on increasing the efficiency of symbolic analysis was demonstrated [10, 12]. Furthermore, the parasitic resistors and capacitors of input-output terminals can be included in the model of an active device to perform symbolic analysis. However, the applied extent of the proposed approaches in [10] is limited because floating pathological element-based active devices cannot be included into the formulation process. In this paper, we intend to present a more comprehensive analytical technique for performing symbolic analysis on the RLC-nullor-floating mirror representation circuits. The proposed approach is applied to two practical circuit examples and some discussions about simplified pathological models of active devices are given.

2 Pathological Sections and Equivalents

The symbols and definitions of the nullor and mirror elements are shown in Table 1. The voltage mirror and current mirror in Tables 1(c) and (d) are lossless two-port network elements used to represent ideal voltage and current reversing property, respectively. Each of the voltage mirror and the current mirror symbols has a reference node, which is set to ground [6]. The symbols and definitions of the floating mirror elements are shown in Tables 1(e)-(f). It can be found that the mirror elements in Tables 1(c) and (d) can be regarded as the special cases of the floating mirror elements in Tables 1(e) and (f), respectively.

In the recent time, the floating mirror elements have been used to represent various popular analog signal-processing properties in concise forms. As shown in Tables 2(a) and (b), two floating voltage mirrors with a common reference node are used to represent the pathological differential voltage cell and differential voltage conveying cell. Also, two floating current mirrors with a common reference node can be used to express the pathological current replication cells as shown in Tables 2(c) and (d) [7]-[8]. From the current replication cell in Table 2(d), it can be found that if the I_x is the input current, the I_y and I_w can be recognized as the output currents of a pathological CM and a norator, respectively. Besides, the constructions in Tables 2(e) and (g) are equivalent to a nullator and a norator, respectively. The constructions in Tables 2(f) and (h) are respectively equivalent to a pathological VM and a CM.

Table 1. Symbols and definitions of nullor and mirror elements

(a)		$V_1 = V_2$ $I_1 = I_2 = 0$
(b)		V_1 and V_2 are arbitrary $I_1 = -I_2 = \text{arbitrary}$
(c)		$V_1 = -V_2$ $I_1 = I_2 = 0$
(d)		V_1 and V_2 are arbitrary $I_1 = I_2 = \text{arbitrary}$
(e)		$V_{13} = -V_{23}$ $(V_1 - V_3 = V_3 - V_2)$ $I_1 = I_2 = 0$
(f)		V_{13} and V_{23} are arbitrary $I_1 = I_2 = I_3/2 = \text{arbitrary}$

The above representation sections are concise comparing with the pathological representations using nullor and mirror elements with grounded reference nodes [13] because they comprise only two floating mirrors without the need of other elements such as resistors. With less internal nodes, the representations in Table 2 are helpful to enhancing the efficiency of symbolic circuit analysis. The sections were used to model some active devices with differential or multiple single-ended features, as shown in Fig. 1. In Fig. 1, it must be noted that the pathological representations of BOCCII and FDCCII are different from the ones in [8] by removing the dummy nullor elements. They can be used for symbolic nodal analysis using the proposed method in Section 3.

Table 2. Some pathological sections and their characteristics

(a) Differential voltage cell		$V_y = V_w - V_x$ $I_w = I_x = I_y = 0$
(b) Differential voltage conveying cell		$V_w - V_x = V_y - V_z$ $I_w = I_x = I_y = I_z = 0$
(c) Current replication cell		$I_z = I_y = -I_x$
(d) Current replication cell		$I_w = I_z = -I_x = -I_y$
(e) Equivalent of nullator		$V_x = V_y$ $I_x = I_y = 0$
(f) Equivalent of VM		$V_x = -V_y$ $I_x = I_y = 0$
(g) Equivalent of norator		$I_y = -I_x$
(h) Equivalent of CM		$I_y = I_x$

3 Symbolic NA of RLC-Nullor-Floating Mirror Network

The steps for symbolic NA of RLC-nullor-floating mirror networks are proposed below. They involve the symbolic nodal analysis of an arbitrary interconnection of RLC-nullor-floating mirror networks and independent current sources in an $(N+1)$ node network (excluding the reference nodes between two mirror elements). The analytic process can be summarized as follows:

Step 1: Select a ground node and label all other nodes from 1 to N except the common reference nodes between two mirror elements (since we do not particularly wish to know the reference node voltages for the floating CMs and the reference node voltages for the floating VMs can be obtained from other node voltages). According to the element properties in Tables 1(b), (d), (f), and 2(c)-(e) denote the currents flow through every norator, current mirror and floating current mirror. It is known that no current flows through the nullators, voltage mirrors and floating voltage mirrors of the network. Also, remember that the sections in Tables 2(f), (g), (h) and (i) are equivalent to a nullator, a VM, a norator and a CM, respectively.

Step 2: Write the nodal admittance equations for every node except the reference nodes between two mirror elements. Express the nodal admittance equations in matrix form:

$$\mathbf{I} = \mathbf{Y}_{N \times N} \mathbf{V} \quad (1)$$

$\mathbf{I} = \{I_1, I_2, \dots, I_N\}'$, where the i th component I_i is defined as the sum of the currents flowing into the i th node from the independent current sources, norators, current mirrors or floating current mirrors. $\mathbf{Y}_{N \times N}$ is the passive nodal admittance matrix. Furthermore, \mathbf{V} is the unknown column vector $\{V_1, V_2, \dots, V_N\}'$ of node voltages.

Step 3: For the floating VM-based sections with three or four ungrounded nodes, i.e., the differential voltage cell in Table 2(a) and the differential voltage conveying cell in Table 2(b), write their relations of nodal voltages and add these equations to (1). Hence the combined equations can be expressed in matrix form $\mathbf{I} = \mathbf{B}\mathbf{V}$. It is clear that each cell adds an additional equation to the combined equations.

Step 4: For a nullator that is connected between the nodes p and q , for example, add the elements of column q to the elements of column p and delete column q of \mathbf{B} . If q is the ground node, simply delete column q of \mathbf{B} . The number of columns of the \mathbf{B} matrix is thereby reduced by one. This operation is based on the voltages at the two terminals of a nullator with respect to the ground node being identical. Thus we can omit one unknown voltage variable in the \mathbf{V} column vector.

Step 5: For a VM that is connected between the nodes r and s , for example, subtract the elements of column s from the elements of column r and delete column s of \mathbf{B} . If s is the ground node, simply delete column r of \mathbf{B} . The number of columns of the \mathbf{B} matrix is thereby reduced by one. This operation is based on the voltage reversing property of a voltage mirror in Table 1(c).

Step 6: For a norator that is connected between nodes l and m , for example, add the equation in row m to the equation in row l and delete row m of the nodal equations. This involves adding I_m to I_l and the m th row of \mathbf{B} to the l th row of \mathbf{B} . If m is the

ground node, simply delete row 1 of the nodal equations. The number of columns of the \mathbf{B} matrix is thereby reduced by one. This operation is based on the current property of a norator in Table 1(b) and the number of equations being enough to solve the unknown independent node voltages after deleting the mentioned equations.

Step 7: For a CM that is connected between the nodes n and o , for example, subtract the equation in row o from the equation in row n and delete row o of the nodal equations. This involves subtracting I_o from I_n and the o th row of \mathbf{B} from the n th row of \mathbf{B} . If o is the ground node, simply delete row n of the nodal equations. This operation is based on the current reversing property of the terminals of a current mirror in Table 1(d) and the number of equations is enough to solve the unknown node voltages.

Step 8: For the pathological current replication cell with three ungrounded nodes x , y and z in Table 2(c), add the equation in row y to the equation in row x ; subtract the equation in row z from the equation in row y and delete row z of the nodal equations. Similar manipulation process can be applied to the cells in Tables 2(d) and (e). This operation is based on the norator behavior between terminals x and y and the CM behavior between terminals y and z . One nodal equation is removed because the number of equations is enough to solve the unknown node voltages.

Step 9: The preceding steps 4-8 incur the reduction of the order of the system of equations derived in step 3. Solve the simplified combined equations for the unknown node voltages in V .

Following the above proposed procedure, it can be observed that each nullator (or VM) will incur the number of columns of the \mathbf{B} matrix is reduced by one and each norator (or CM) will incur the number of rows of the \mathbf{B} matrix is reduced by one. In Tables 2(a) and (b), it should be noted that each pathological section will result in the number of rows of the \mathbf{B} matrix is increased by one and they cannot reduce the number of columns of the \mathbf{B} . In addition, in Tables 2(c)-(d), each pathological section will result in the number of rows of the \mathbf{B} matrix is reduced by one. Let us review the pathological models of active devices in Fig. 1. It can be found that the active devices models in Fig. 1 will incur the identical number of rows and columns of the \mathbf{B} matrix. Hence the resulting matrix will still be square and hence solvable. So the pathological models in Fig. 1 can be used for the proposed symbolic NA approach.

4 Application Example

To demonstrate the feasibility of the proposed models and the symbolic NA method in Section 3, practical circuit example is illustrated. For comparison with previous techniques, we adopt the same circuit example as the second example in [13]. It is a DDCC+-based design in Fig. 2(a) of [14]. Fig. 2 shows its pathological representation with the equivalence of the inputted voltage source [15]. As shown in Fig. 2, the DDCC+ is modeled by using the pathological differential voltage conveying cell in Table 2(b) and a CM. Based on steps 1-3 of the proposed symbolic NA, we can write the (6×5) nodal admittance equations in matrix form $\mathbf{I} = \mathbf{BV}$ as

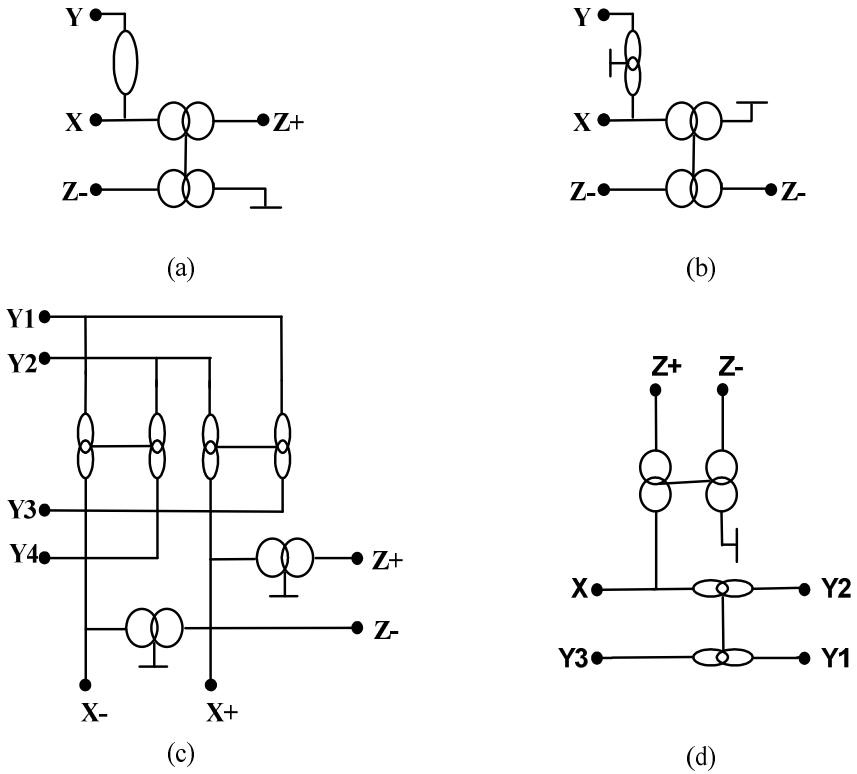


Fig. 1. Nullor-floating mirror models. (a) BOCCII (b) DOICCCII-- (c) FDCCII (d) DDCC

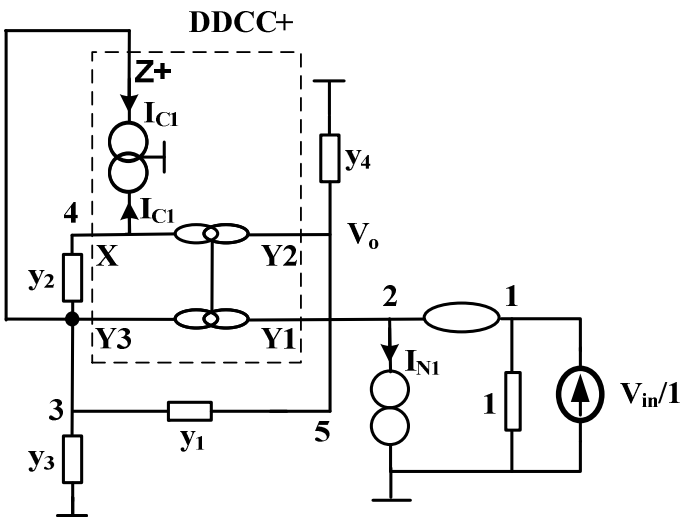


Fig. 2. DDCC+-based voltage-mode biquad filter

$$\begin{bmatrix} V_{in} / 1 \\ I_{N1} \\ I_{C1} \\ I_{C1} \\ 0 \\ 0 \end{bmatrix} = \begin{bmatrix} 1 & 0 & 0 & 0 & 0 \\ 0 & 0 & 0 & 0 & 0 \\ 0 & 0 & y_1 + y_2 + y_3 & -y_2 & -y_1 \\ 0 & 0 & -y_2 & y_2 & 0 \\ 0 & 0 & -y_1 & 0 & y_1 + y_4 \\ 0 & -1 & -1 & 1 & 1 \end{bmatrix} \begin{bmatrix} V_1 \\ V_2 \\ V_3 \\ V_4 \\ V_5 \end{bmatrix} \tag{2}$$

After applying the steps 4-8 of the proposed method leads to the derivation of the following (4 × 4) combined equations as (3). The output transfer function can be obtained and given in (4). The analyzed results are in accordance with the circuit functions in [14]. So the feasibility of the proposed method is verified. In addition, in this example the built symbolic matrix of dimension is (6 × 5) and it is reduced to (4 × 4) with 10 nonzero coefficients as in (3). Compared to the symbolic NA approach using nullor-mirror model of DDCC+ (as shown in Fig. 5 of [13]), the built symbolic matrix of dimension is (9 × 9) and it is reduced to (5 × 5) with 13 nonzero coefficients. So it reveals the improvement of this proposed approach.

$$\begin{bmatrix} V_{in} / 1 \\ 0 \\ 0 \\ 0 \end{bmatrix} = \begin{bmatrix} 1 & 0 & 0 & 0 \\ 0 & y_1 + 2y_2 + y_3 & -2y_2 & -y_1 \\ 0 & -y_1 & 0 & y_1 + y_4 \\ -1 & -1 & 1 & 1 \end{bmatrix} \begin{bmatrix} V_{1,2} \\ V_3 \\ V_4 \\ V_5 \end{bmatrix} \tag{3}$$

$$\frac{V_5}{V_{in}} = \frac{V_o}{V_{in}} = \frac{2y_1y_2}{2y_1y_2 + y_1y_4 + y_1y_3 + y_3y_4} \tag{4}$$

5 Conclusion

In this paper, an efficient symbolic NA technique using of any pathological elements is proposed. Some pathological representations of active devices are modified by omitting the dummy pathological elements to perform symbolic NA. The simplified models with less internal nodes are conducive to enhancing the analysis efficiency. Practical application example is given which demonstrate the workability of the proposed symbolic NA approach.

Acknowledgments. This work has been supported by the National Science Council of the Republic of China (Grant Nos NSC 101-2221-E-151-074).

References

1. Tellegen, B.D.H.: La recherche pour une série complète d'éléments de circuit idéaux nonlinéaires. *Rendiconti del Seminario Matematico e Fisico di Milano* 25, 134–144 (1954)
2. Carlin, H.J.: Singular network elements. *IEEE Trans. Circuit Theory* CT-11, 67–72 (1964)
3. Schmid, H.: Approximating the universal active element. *IEEE Trans. Circuits Syst. II* 47(11), 1160–1169 (2000)
4. Carlosena, A., Moschytz, G.S.: Nullators and norators in voltage to current mode transformations. *Int. J. Circuit Theory Applicat.* 21(4), 421–424 (1993)
5. Kumar, P., Senani, R.: Bibliography on nullors and their applications in circuit analysis, synthesis and design. *Anal. Integr. Circuits Signal Process.* 33(1), 65–76 (2002)
6. Soliman, A.M., Saad, R.A.: The voltage mirror-current mirror pairs as a universal element. *Int. J. Circuit Theory Appl.* 38(8), 787–795 (2010)
7. Saad, R.A., Soliman, A.M.: On the systematic synthesis of CCII-based floating simulators. *Int. J. Circuit Theory Appl.* 38(9), 935–967 (2010)
8. Saad, R.A., Soliman, A.M.: A new approach for using the pathological mirror elements in the ideal representation of active devices. *Int. J. Circuit Theory Appl.* 38(2), 148–178 (2010)
9. Soliman, A.M.: Pathological representation of the two-output CCII and ICCII family and application. *Int. J. Circuit Theory Appl.* 39(6), 589–606 (2011)
10. Sanchez-Lopez, C., Fernandez, F.V., Tlelo-Cuautle, E., Tan, S.X.D.: Pathological element-based active device models and their application to symbolic analysis. *IEEE Trans. Circuits Syst. I: Reg. Papers* 58(6), 1382–1395 (2011)
11. Tlelo-Cuautle, E., Sanchez-Lopez, C., Moro-Frias, D.: Symbolic analysis of (MO)(I) CCI(II)(III)-based analog circuits. *Int. J. Circuit Theory Appl.* 38(6), 649–659 (2010)
12. Wang, H.Y., Huang, W.C., Chiang, N.H.: Symbolic nodal analysis of circuits using pathological elements. *IEEE Trans. Circuits Syst. II* 57(11), 874–877 (2010)
13. Huang, W.C., Wang, H.Y., Cheng, P.S., Lin, Y.C.: Nullor equivalents of active devices for symbolic circuit analysis. *Circuits Syst. Signal Process.* 31, 865–875 (2012)
14. Ibrahim, M.A., Kuntman, H., Cicekoglu, O.: New second-order low-pass, high-pass and band-pass filters employing minimum number of active and passive elements. In: *Proc. Int. Symp. Signal Circuits Syst.*, pp. 557–560 (2003)
15. Svoboda, J.A.: A linear active network analysis program suitable for a class project. *IEEE Trans. Education* E-27(1), 21–25 (1984)